

# Passive vs. Parachute System Architecture for Robotic Sample Return Vehicles

**Robert Maddock**  
 NASA Langley Research Center  
 1 N. Dryden St., M.S. 489  
 Hampton, VA 23681  
 757-864-7353  
 robert.w.maddock@nasa.gov

**Allen Henning**  
 Virginia Tech  
 103 K Stratford Dr.  
 Williamsburg, VA 23188  
 757-345-1155  
 allenhenning3@vt.edu

**Jamshid Samarah**  
 NASA Langley Research Center  
 1 N. Dryden St., M.S. 451  
 Hampton, VA 23681  
 757-864-5776  
 jamshid.a.samareh@nasa.gov

*Abstract*— The Multi-Mission Earth Entry Vehicle (MMEEV) is a flexible vehicle concept based on the Mars Sample Return (MSR) EEV design which can be used in the preliminary sample return mission study phase to parametrically investigate any trade space of interest to determine the best entry vehicle design approach for that particular mission concept. In addition to the trade space dimensions often considered (e.g. entry conditions, payload size and mass, vehicle size, etc.), the MMEEV trade space considers whether it might be more beneficial for the vehicle to utilize a parachute system during descent/landing or to be fully passive (i.e. not use a parachute).

In order to evaluate this trade space dimension, a simplified parachute system model has been developed based on inputs such as vehicle size/mass, payload size/mass and landing requirements. This model works in conjunction with analytical approximations of a mission trade space dataset provided by the MMEEV System Analysis for Planetary EDL (M-SAPE) tool to help quantify the differences between an active (with parachute) and a passive (no parachute) vehicle concept.

Preliminary results over a range of EEV and mission constraints (including entry conditions, vehicle size, payload mass, and landing requirements) are provided. For most sample return missions, the landing requirement (velocity and/or load) is ultimately determined by science considerations (e.g. sample preservation or containment). Regions of the trade space are identified where a parachute system is clearly more beneficial than the passive approach, and vice versa. Where the choice between the two architectures is less clear, additional considerations must also be taken into account including factors such as overall system reliability; system risk and complexity; and development and testing costs.

## TABLE OF CONTENTS

1. INTRODUCTION.....	1
2. THE MULTI-MISSION EARTH ENTRY VEHICLE ...	1
3. PURPOSE.....	2
4. MMEEV SYSTEM ANALYSIS FOR PLANETARY ENTRY, DESCENT AND LANDING.....	2
5. PARACHUTE MODELING .....	5
6. PASSIVE VERSUS PARACHUTE .....	6
7. OTHER CONSIDERATIONS.....	7
8. CASE STUDY.....	8
9. CONCLUSIONS AND FUTURE WORK.....	9
SYMBOLS AND NOTATION.....	9
ACKNOWLEDGEMENTS .....	9

REFERENCES.....	9
BIOGRAPHIES.....	10

## 1. INTRODUCTION

The Multi-Mission Earth Entry Vehicle (MMEEV) is a flexible vehicle concept, based on the Mars Sample Return (MSR) Earth Entry Vehicle (EEV) design [1], which can be used in the preliminary study phase of any sample return mission concept (e.g. lunar, asteroid, comet, or planetary) and later optimized to meet that mission’s specific requirements. The interest of the research described here is to quantitatively and qualitatively compare a fully passive architecture to the more historical approach of relying on a parachute system. It can be shown that there will always be times when a parachute is absolutely necessary, particularly when low landing velocities are required. However, if the landing load requirement (which is typically driven by science considerations) is allowed to increase, a passive vehicle approach may be more beneficial.

To fully understand this trade, a simplified parachute system mass model was developed to understand, to first order, the mass which must be added to a comparable passive MMEEV concept to meet these lower landing velocity requirements. An analysis of a mission and vehicle trade space also provides a more efficient technique for sizing of the passive MMEEV concepts across a wide range of desired inputs. These quantitative models are then used to develop a comparison between passive and active EEV architectures.

## 2. THE MULTI-MISSION EARTH ENTRY VEHICLE

The Multi-Mission Earth Entry Vehicle (MMEEV) concept began as an internal NASA Langley Research Center development in 2006 as a follow-up to the work done in support of MSR for the Mars Technology Program [2]. From 2008-2013, NASA’s In-Space Propulsion Technology Development Program directed the development of the concept [3,4]. Since 2013, NASA Langley and Ames Research Centers have provided internal resources to further development of MMEEV concept in support of risk mitigation activities, particularly in understanding structural hardware manufacturing limitations, performance verification testing and vehicle integration. The MMEEV

design concept has also been utilized in various sample return mission studies and mission proposals [5].

The highly reliable MSR EEV concept provides a logical foundation upon which any sample return mission can build an optimized EEV design to meet their specific needs. By preserving key design elements, the MMEEV concept provides a platform by which key technologies can be identified, designed, developed, and flight-proven prior to implementation on a MSR mission. By utilizing this shared, flexible design concept, any sample return mission can benefit from the technology developments and flight experience of previous MMEEV designs, resulting in reduced risk and lower development costs.

### 3. PURPOSE

One of the most critical phases of any sample return mission is the atmospheric entry and descent at Earth. A sample return vehicle must be able to protect the sample while traveling through the Earth’s atmosphere and land on the ground without loss of integrity (i.e. science value) of the sample. Sample containment (i.e. from the Earth’s biosphere) may also be important when returning a sample from a location where there is little understanding of the possible hazards related to exposure of the sample to life on Earth. Missions such as these (e.g. MSR) may require extremely high system reliability, with a chance of mission failure on the order of one-in-a-million or lower.

When it comes to considering the architecture of the entry, descent, and landing (EDL) phase of a sample return capsule, there are two diametric approaches worth considering. First is the heritage approach of a utilizing a parachute system to help decelerate the vehicle (and payload) to the desired landing speed. This parachute system generally includes not only a main canopy, but also a deployment system (i.e. mortar and/or a pilot parachute), and possibly even a drogue parachute to increase aerodynamic stability. In addition, parachute deployment and peak inflation loads must be considered when sizing the vehicle structure, and mass necessary for the parachute deployment system should also be included as part of the parachute system mass estimate.

The second approach to consider is a fully passive vehicle with no additional aerodynamic deceleration beyond that provided by the drag of the entry vehicle itself. This approach relies on some form of impact or energy attenuation to meet the payload landing constraints upon contact with the surface. Depending on the landing site, some impact attenuation can potentially be provided by the soil itself instead of an on-board system. Analyzing and understanding the quantitative and qualitative aspects of both of these architectures is the main purpose of this study.

## 4. MMEEV SYSTEM ANALYSIS FOR PLANETARY ENTRY, DESCENT AND LANDING

The MMEEV System Analysis for Planetary EDL (M-SAPE) trade space analysis tool [6] has been developed to provide guidance in selecting a preliminary MMEEV design based on a range of input parameters, such as entry velocity, entry flight path angle, Thermal Protection System (TPS) material, vehicle diameter, payload mass (which includes the sample itself, the sample container and any sample monitoring or environmental control hardware), desired landing load, etc. Input parameters can be varied across a range, in which case the tool provides a large dataset summarizing all viable concepts and their performance across the desired trade space. Mass estimation relationships (MERs) can then be derived from this dataset that allow for a rapid and more complete analysis of the trade space without relying on computational resources and time required for the M-SAPE tool itself.

For this study, a M-SAPE dataset was generated in order to determine MERs relating the vehicle entry mass and impact system mass to payload mass, payload density, vehicle diameter<sup>1</sup>, and landing load, by varying those parameters (across all combinations) from 5 to 35 kg (in 5 kg increments), 2000 to 6000 kg/m<sup>3</sup> (in 500 kg/m<sup>3</sup> increments), 0.6 to 1.8 m (in 0.2 m increments) and 500 to 2500 g (in 250 g increments) respectively. All other input parameters were fixed at values meant to be representative of typical EEV designs. A summary of the more critical of these values is provided in Table 1. The M-SAPE output dataset was then analyzed to derive MERs for vehicle entry mass and impact system mass as a function of those variables.

**Table 1. Fixed Input Values used for M-SAPE Dataset**

Input Parameter	Value
Input Shoulder Radius / Vehicle Radius	0.05
Nose Radius / Input Vehicle Radius	0.782
Entry Velocity	12.0 km/s
Entry Flight Path Angle	-8.0°
Aftbody TPS Concept	Acusil
Mass Margin	30%
Mass Convergence Criterion	0.001 kg
Max Number of Iterations	20
Forebody TPS	PICA
Carrier Structure Concept	AL-5056
Convective Heat Rate Model	Sutton-Graves
Convective Heat Rate Margin	1.3
Radiative Heat Rate Model	Tauber-Sutton
Radiative Heat Rate Margin	1.0
Impact Foam Stroke Efficiency	80%
Impact Foam Stroke Margin	20%

<sup>1</sup>If the inputs are such that the vehicle diameter provided is too small for the parametric vehicle model to close geometrically (e.g. a very large payload size with a very small vehicle diameter), the M-SAPE tool will determine the minimum diameter that allows for convergence while all other vehicle inputs and/or constraints to be met.

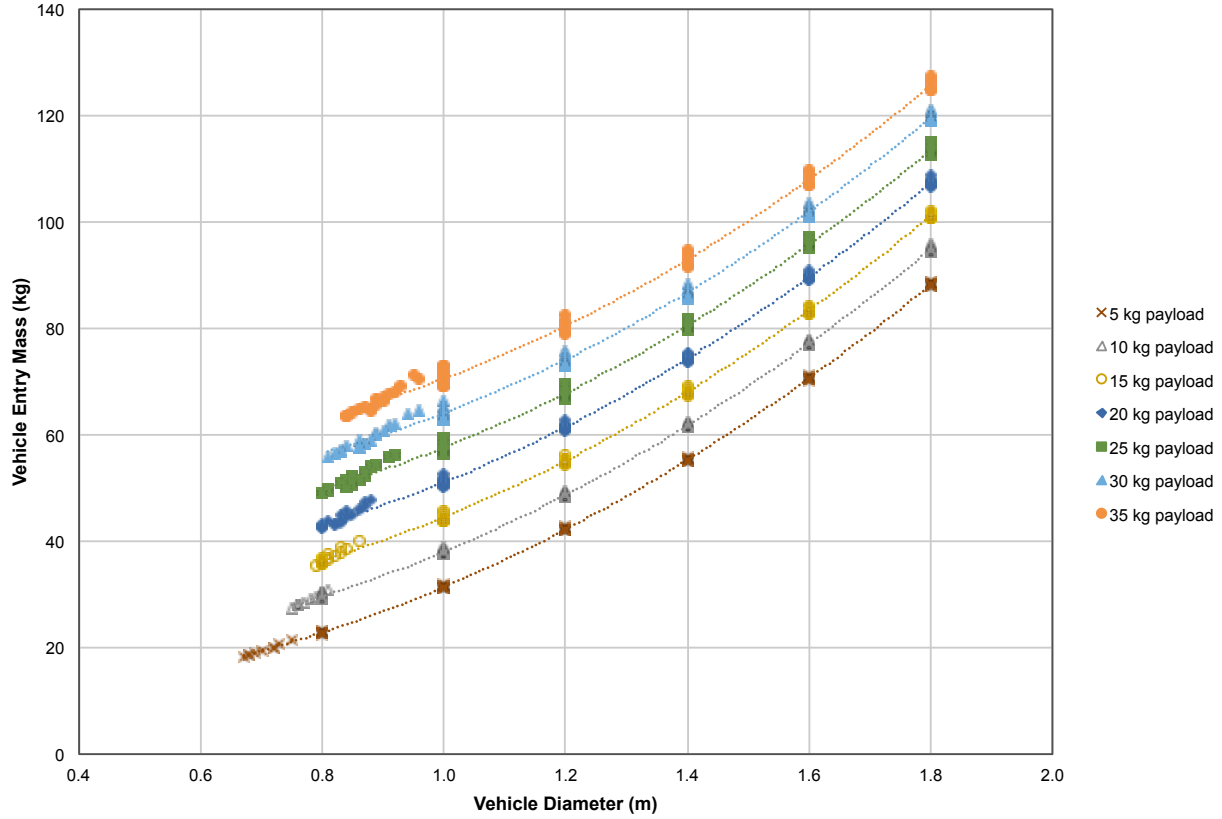


**Figure 1. Entry Mass vs. Vehicle Diameter for a 1500 g Landing Load**

Figure 1 illustrates the relationship between the MMEEV entry mass, vehicle diameter and payload mass for a 1500 g landing load using the M-SAPE dataset. The multiple data points at each diameter for a specified payload mass shows the effect of payload density. Although the payload density plays a part in the impact system mass (in the determination of the required stroke, or compression of the impact system, necessary to achieve a required landing load), it does not appear to be a major contributor to the overall vehicle entry mass. Therefore, a payload density of 6000 kg/m<sup>3</sup> was used throughout the remainder of this study to provide a more conservative impact system mass (i.e. a higher density would result in a longer stroke required to meet a given landing load, therefore a higher impact system mass).

Plots of vehicle entry mass versus vehicle diameter for the various payload masses were created for landing loads ranging from 500 to 2500 g's. For each landing load, various curve fits (e.g. linear, polynomial, exponential, etc.) were applied to see which form provided the best fit (i.e. maximizes the R-squared value). In this case, it was determined that the entry mass of the passive vehicle ( $m_{e_{passive}}$ ) can be best estimated as a quadratic function of vehicle diameter ( $D_v$ ) for each payload mass:

$$m_{e_{passive}} = A \cdot D_v^2 + B \cdot D_v + C \quad (1)$$

The values of the coefficients A, B and C were then plotted as a function of the payload mass ( $m_{pay}$ ), and similarly,

applying various curve fits showed that they can be estimated as a quadratic function, e.g.:

$$A = D \cdot m_{pay}^2 + E \cdot m_{pay} + F \quad (2)$$

and where the coefficients D, E, and F were similarly related to the landing load ( $l_i$ ) using a quartic fit, e.g.:

$$D = \alpha \cdot l_i^4 + \beta \cdot l_i^3 + \gamma \cdot l_i^2 + \delta \cdot l_i + \epsilon \quad (3)$$

where  $\alpha$ ,  $\beta$ ,  $\gamma$ ,  $\delta$ , and  $\epsilon$  are constants determined from the curve fits. This MER provides values of vehicle entry mass within ~0.5% of the dataset provided by the M-SAPE tool.

This same approach was used for estimating the MMEEV impact system mass. After a series of fitting exercises, considering various combinations of inputs and constraints, a relationship between the vehicle diameter and the inverse of the impact system mass fraction (ratio of vehicle entry mass to the impact system mass), as illustrated in Figure 2 for a 1500 g landing load, appeared to show the best correlation. For each landing load and payload mass, a quadratic fit was used to estimate this mass ratio as a function of vehicle diameter:

$$\left(\frac{m_e}{m_{is'}}\right)_{passive} = A \cdot D_v^2 + B \cdot D_v \quad (4)$$

where the coefficients A can be estimated using a power function and B using a cubic function of payload mass:

$$A = C \cdot m_{pay}^D \quad (5)$$

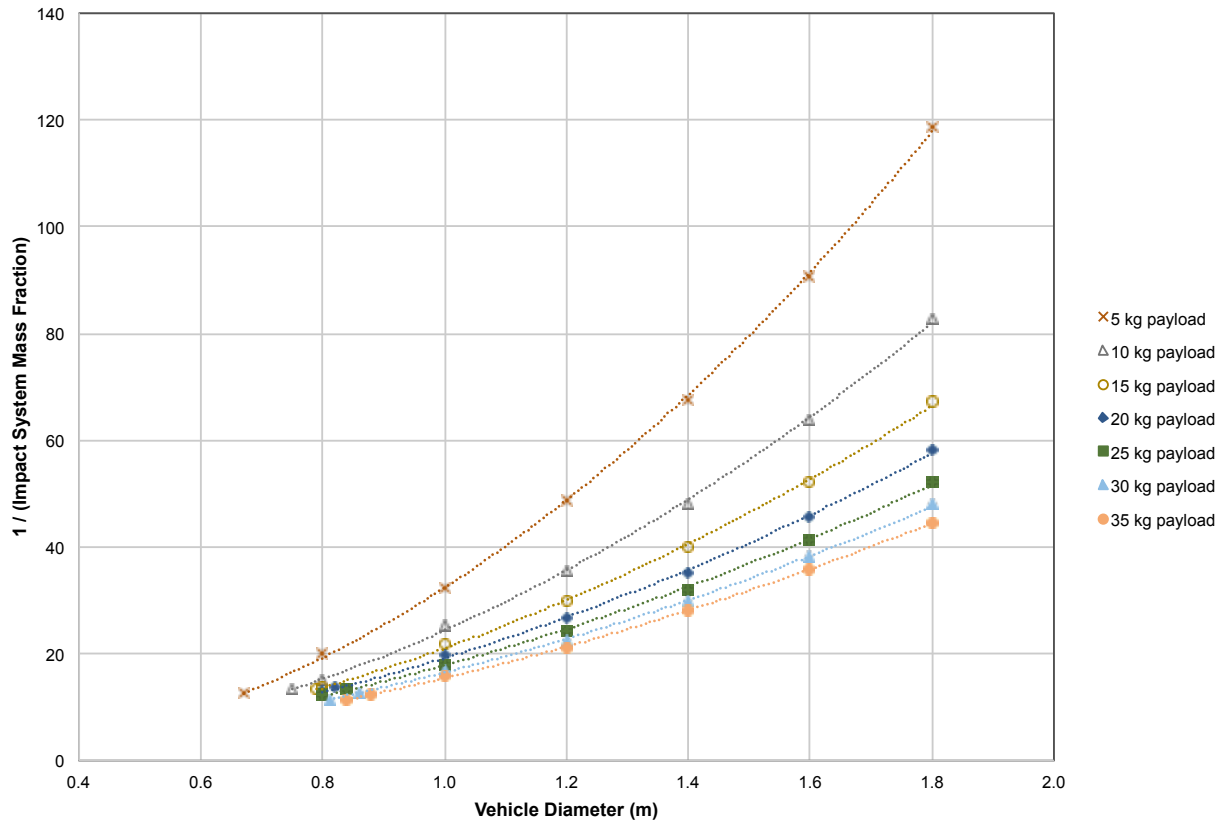


Figure 2. Inverse of Impact System Mass Fraction vs. Vehicle Diameter and Payload Mass for a 1500 g Landing Load

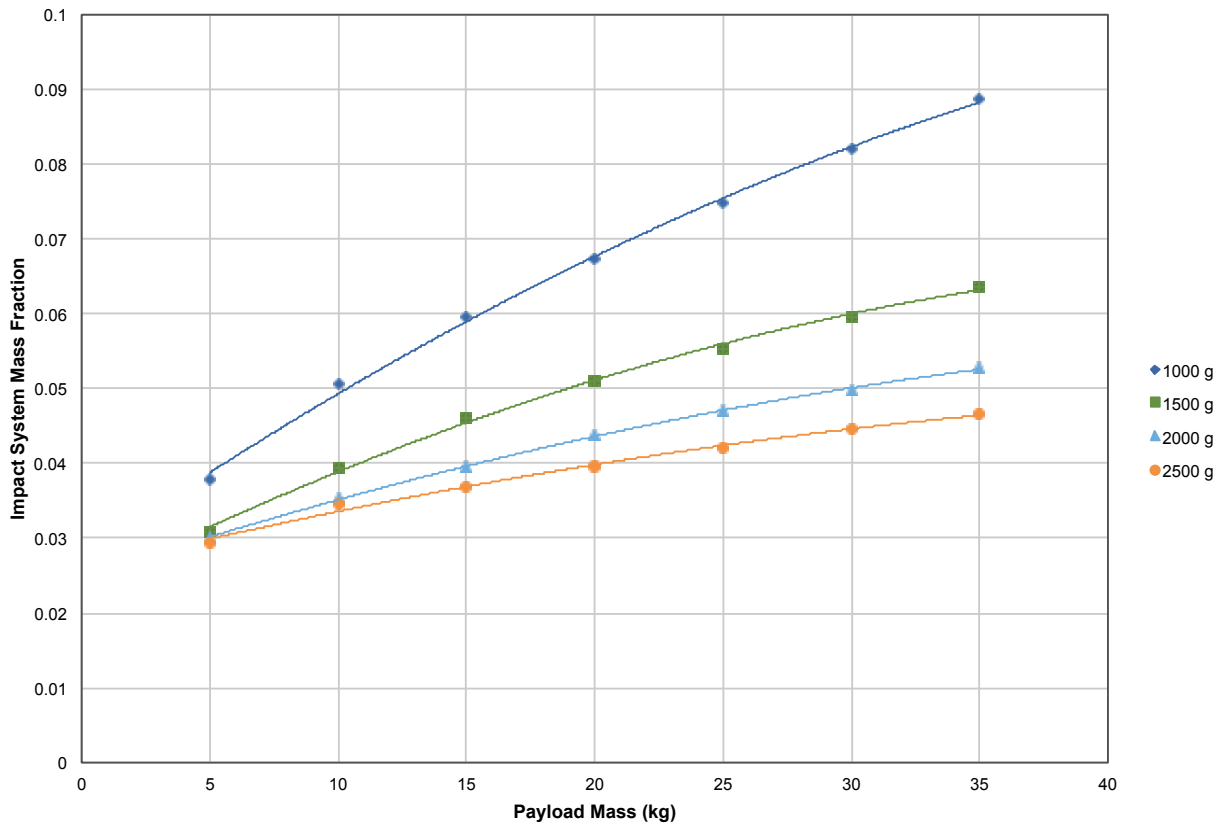


Figure 3. Impact System Mass Fraction vs. Payload Mass and Landing Loads for a 1m Diameter Vehicle

$$B = E \cdot m_{pay}^3 + F \cdot m_{pay}^2 + G \cdot m_{pay} + H \quad (6)$$

and where the coefficients C can be estimated using an exponential function and D using a linear function of the landing load:

$$C = \alpha \cdot e^{\beta \cdot l_i} \quad (7)$$

$$D = \gamma \cdot l_i + \delta \quad (8)$$

and where the coefficients E, F, G and H were estimated as a cubic function of the landing load, e.g.:

$$E = \varepsilon \cdot m_{pay}^3 + \mu \cdot m_{pay}^2 + \omega \cdot m_{pay} + \theta \quad (9)$$

where  $\alpha$ ,  $\beta$ ,  $\gamma$ ,  $\delta$ ,  $\varepsilon$ ,  $\mu$ ,  $\omega$ , and  $\theta$  are constants determined from the curve fits. Using this MER for the impact system mass provides values within ~6% of the dataset provided by the M-SAPE tool.

Based on this MER (Eq. 4), Figure 3 takes a different look at the sensitivity of the impact system mass as a function of the payload mass and landing load requirement for a representative 1 m diameter vehicle. Not surprisingly, the impact system for the passive vehicle appears to be modestly sensitive to the payload mass. For the passive approach, M-SAPE sizes the impact system as a solid foam energy absorber which is used in conjunction with impacting an infinitely hard surface, an assumption also used for the original MSR EEV [7]. However, unlike MSR, M-SAPE further assumes that the energy absorber is required to attenuate the kinetic energy of the payload only rather than that of the entire vehicle. This allows for a simple one-dimensional energy balance to be used. The stroke of the impact system required to achieve the desired load is then directly related to the payload mass (and size, or density) and the velocity of the payload system at the time of impact, which in turn is a function only of the vehicle terminal velocity (mass, diameter and vehicle shape).

It is also important to note that depending on the impact speed, soil conditions, and kinetic energy of the vehicle at the time of impact, other energy attenuation concepts, not considered in the current M-SAPE model, could be more mass efficient than the crushable approach described here. In fact, for some impact conditions (e.g. landing in wet clay, which is the predominant soil type at the Utah Test and Training Range, UTTR), and when assuming a highly rigid vehicle, it is probable that the payload support structure will not be required to crush at all in order to meet some landing load requirements since deceleration can be achieved solely through ground penetration of the vehicle itself [8].

## 5. PARACHUTE MODELING

For the purpose of this analysis, a simplified low-fidelity parachute system mass model was needed to estimate the parachute system mass as a function of the desired landing velocity. This model accounts for a main parachute (which includes the canopy, riser and suspension lines, confluence

fittings, etc.), a drogue parachute to provide transonic stability and to deploy the main parachute<sup>2</sup>, and a mortar for deploying the drogue. Assuming a nylon recovery parachute type [9], and a drag coefficient of 0.85 as representative of likely parachute geometries for MMEEV applications [10], a simple linear relationship (Figure 4) between the reference drag area of the parachute ( $C_d S$ ) and the mass of the main parachute ( $m_{mp}$ ), can be estimated as:

$$m_{mp} = 1.05 \cdot (0.08 \cdot (C_d S)) \quad (10)$$

where the 1.05 factor is used to account for the additional mass of the parachute deployment bag.

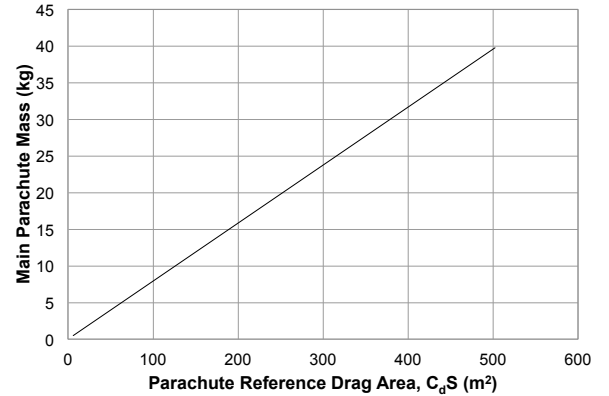


**Figure 4. Main Parachute Mass vs. Parachute Reference Drag Area ( $C_d S$ )**

The required drag area of the main parachute can be expressed as a function of the desired terminal (landing) velocity, minus the drag contribution of the suspended vehicle:

$$(C_d S)_{mp} = \frac{2 \cdot m_v \cdot g}{\rho \cdot v_{term}^2} - (C_d S)_v \quad (11)$$

Historically, the drogue parachute mass ( $m_d$ ) weighs 25-40% of the main parachute, depending on the deployment dynamic pressure and riser length [11]. Based on this, 25% (which also accounts for the drogue deployment bag) was assumed for this model to provide an optimistic parachute system mass:

$$m_d = 0.25 \cdot m_{mp} \quad (12)$$

The mass of the mortar system ( $m_m$ ) used to deploy a drogue parachute was also estimated based on historical data [12]:

$$m_m = 2.2 \cdot (m_d)^{0.5} \quad (13)$$

The total parachute system mass ( $m_{ps}$ ) therefore becomes:

$$m_{ps} = m_{mp} + m_d + m_m \quad (14)$$

<sup>2</sup> Since the parachute system is typically packaged towards the aft of the vehicle, the center of gravity of the EEV will also be shifted aft, resulting in a decrease in transonic/subsonic aerodynamic stability. In this case, a drogue parachute would be used to stabilize the vehicle prior to main parachute deployment.

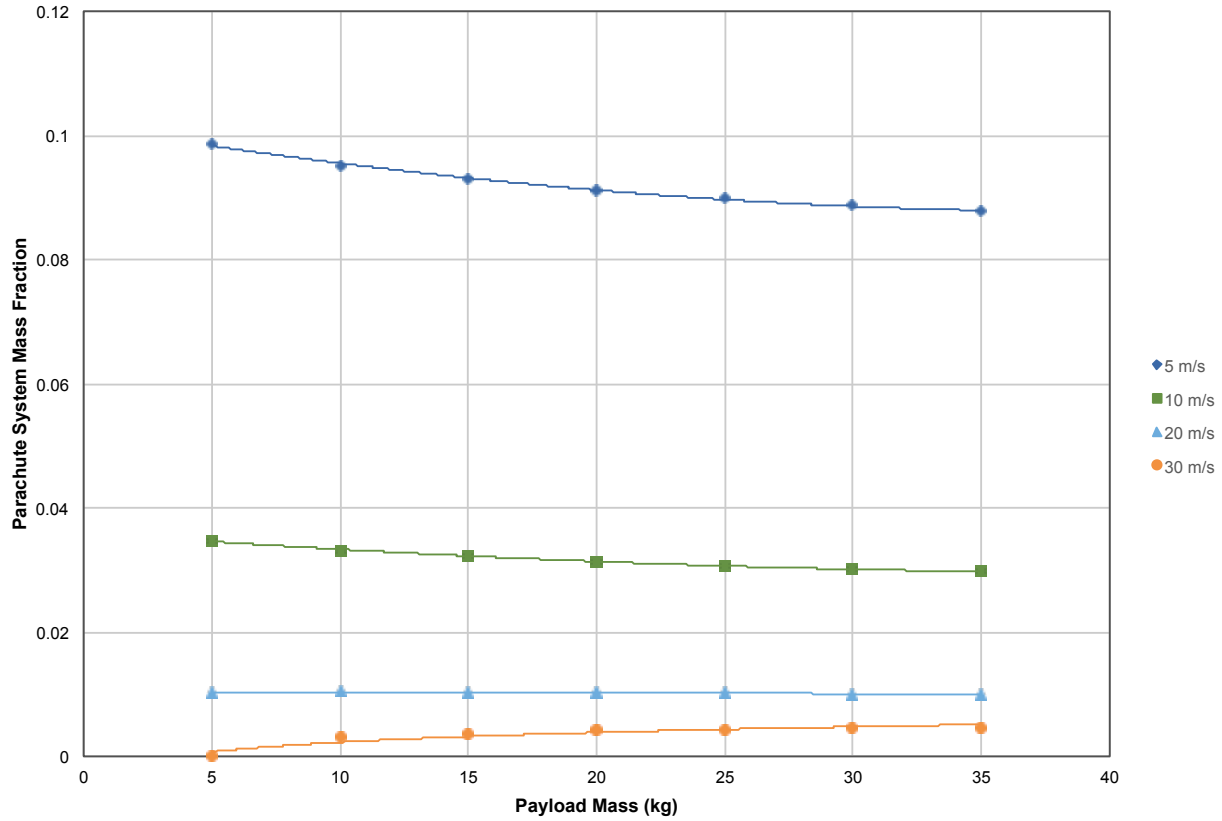


**Figure 5. Parachute System Mass Fraction vs. Payload Mass and Landing Velocity for a 1 m Diameter Vehicle**

Based on this MER, the parachute system mass fraction (parachute system mass / total entry mass) for the active vehicle architecture appears to be relatively insensitive to a change in payload mass, as shown in Figure 5. For this architecture, a change in payload mass only affects the suspended vehicle mass on the parachute. Since the terminal velocity (or landing velocity) is dominated by the drag of the parachute, which is a much more highly efficient drag device than the vehicle itself, a small change in payload mass can be accommodated for by a very small change in parachute size and mass.

## 6. PASSIVE VERSUS PARACHUTE

Using the MERs developed for both the passive and parachute architectures, total vehicle entry mass estimates were generated for configurations across the input parameters of interest (vehicle diameter, landing load or velocity, and payload mass). For the passive vehicle, the MERs can be used directly to determine the entry mass for each set of conditions and desired landing load. To calculate the analogous active vehicle mass, the impact system mass would be subtracted from the passive vehicle entry mass (except for a small amount – no more than 2 kg – to account for a payload support structure) and the parachute system mass for the desired landing velocity is added:

$$m_{e_{active}} = (m_{e_{passive}} - m_{is}) + m_{ps} \quad (15)$$

It is important to remember that this parachute system mass is added to the vehicle mass without consideration of the additional volume that may be required, the additional structural mass needed to accommodate that added volume as well as the parachute peak inflation load, or any additional subsystem mass needed to deploy the parachute system. The consideration of these details were beyond the scope of this study. However, it is safe to say that when considering these additional mass impacts, the utilization of a parachute system would only appear to be “less attractive”, except for those cases where it is absolutely necessary.

When considering a way to quantify the comparison between the passive versus active, or parachute, architecture, one metric chosen to investigate was the payload mass fraction (the ratio of payload mass to vehicle entry mass). This metric provides a means of illustrating how much of the MMEEV total entry mass can be allocated to the payload system, and thus, the sample (or the science) itself. An example of this is shown in Figure 6 for a 15 kg payload. Contours of various landing velocities are shown for the active vehicle while the various landing loads are shown for the passive vehicle. (It is important to note that the landing velocity for a passive vehicle with a given landing load is a function of vehicle diameter, so the comparisons made in Figure 6 are not direct. However, for reference, the landing velocity for the passive vehicle data shown ranges from approx. 30-40 m/s.) Based on these

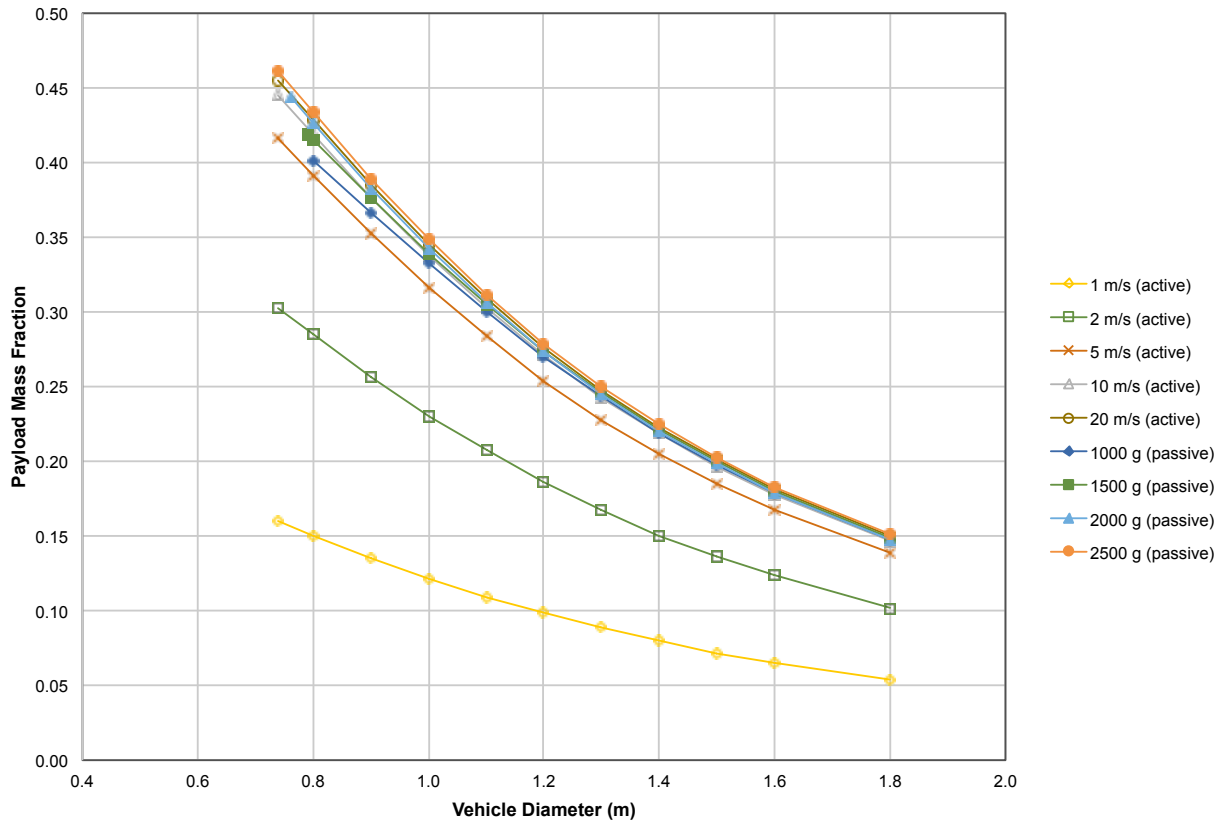


**Figure 6. Payload Mass Fraction vs. Vehicle Diameter and Landing Conditions for a 15 kg Payload**

results, if the desired landing velocity was on the order of 5 m/s or less, clearly a parachute would be required. However, if the landing velocity of the active vehicle is allowed to increase, the parachute system mass decreases, eventually reaching the same order as the comparable impact system, at which point the payload mass fraction becomes the same as that of the passive vehicle.

Also note that there appears to be little impact on the passive vehicle payload mass fraction as a function of landing load. This follows from Figure 2, which shows that the impact system mass, when compared to the overall entry mass of the passive vehicle, is relatively small, regardless of the landing load. In other words, the M-SAPE impact system model can account for large variations in landing load, for a given payload mass, with very small variations in impact system mass (i.e. small changes in the required stroke). Given these results, it seems reasonable to expect that if the landing load is allowed (by the science team) to be on the order of 1000 g or higher, the passive approach may be more beneficial with respect to payload mass fraction. These results also illustrate, however, that if landing between approximately 10 m/s and 1000 g, there appears to be little difference in the payload mass fraction between the passive and active architectures.

## 7. OTHER CONSIDERATIONS

For the range in the desired landing conditions where payload mass fraction points to either the passive or active concept as being viable, other considerations must be taken into consideration before selecting an architecture.

One such consideration is the sensitivity of each architecture to external environmental effects, such as atmospheric and wind conditions. This becomes important in understanding the landing footprint, which can directly relate to the ability to locate and retrieve the vehicle and sample in a timely manner. Figure 7 illustrates this effect, comparing the expected landing footprint for a passive and active vehicle with the same vehicle diameter and payload mass (assuming an Earth GRAM 2010 atmosphere and winds [13]).

Another important consideration is vehicle configuration (or complexity). When adding a parachute system to a sample return vehicle, the packaging of the parachute and its location relative to the payload system must account for the need to access the payload in order to insert the science samples prior to release of the EEV back at Earth. These two systems, each accounting for a significant fraction of the overall vehicle mass, could result in a complex configuration and/or concept of operations for the sample insertion process.

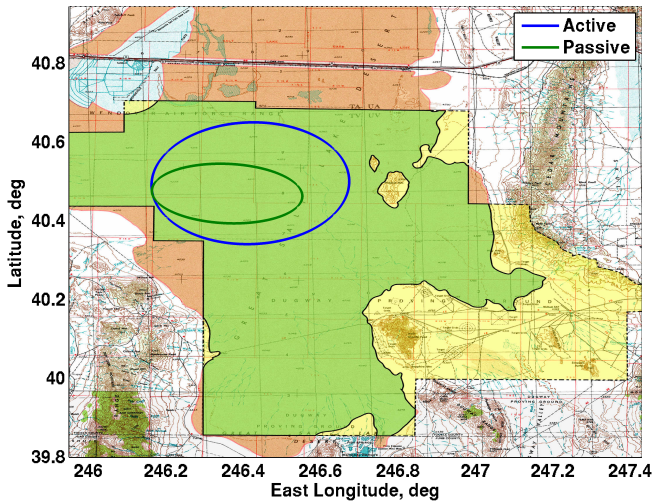


**Figure 7. Landing Footprint (99-percentile) for 1.2 m Diameter Passive (1500 g) and Active (5 m/s) Vehicles with a 20 kg Payload**

System reliability can also differ between passive and active vehicles. With a fully passive vehicle, since there are no active systems onboard to contend with, system reliability is driven by only passive systems (e.g. structures) and additional environmental considerations (e.g. atmospheric knowledge), with the main focus being on survivability or sample preservation upon impact. An active vehicle, however, must also rely on one or more additional systems to perform as designed in order to successfully complete EDL. The parachute system relies on a series of events (e.g. sensors and command triggers, pyro initiations, deployments, etc.) that must all be successful for the parachute to perform as required. In addition, a power source (for sensors and pyros) and a flight processor (for command and data handling) would also be necessary to coordinate these events. With each event/component having a finite probability of failure, the series of events combine to decrease the overall reliability of parachute system, and thus the vehicle as a whole.

Table 2 summarizes one example of the overall reliability of a generalized parachute system [14]. These values assume the use of three pyrotechnics to eject the cover, a single drogue parachute, and a single main parachute. An additional 0.0001 was also subtracted from each event to account for the reliability of a signal being sent from/received by the appropriate sensors/actuator.

**Table 2. Reliability Associated with Parachute System Deployment Sequence**

Event	Reliability
Cover Ejected	0.9996
Drogue Deployed	0.9998
Main Chute Deployed (with drogue)	0.9998
Main Chute Deployed (w/o drogue)	0.99
SRC and Canister Found	0.99999
Overall Reliability	0.9892

For most sample return missions, this level of reliability would be acceptable. However, in cases such as MSR, where planetary protection concerns drive the need for extreme system reliability, even these high reliabilities would be insufficient. The issue of system reliability must be considered along with other factors, such as overall system complexity, development and testing costs, and even the concept of operations for the vehicle. Clearly, none of these factors can be taken singularly. The impact of each of these architectures on the MMEEV system as a whole must be considered before making a selection.

## 8. CASE STUDY

As a means of further quantifying differences between the passive and active MMEEV approach, a case study was used to compare both against a previously flown active EEV design, the Stardust Sample Return Capsule (SRC), using a fixed vehicle diameter and payload mass<sup>3</sup> (see Table 3).

One thing to note from this case study is that, given the same landing velocity, vehicle diameter and payload mass, the parachute system model described above does provide an accurate estimate of the parachute system mass when compared to the Stardust SRC (within ~3%). The difference in entry mass between the active case and the Stardust reference is due to multiple factors, including differences in the primary structural configuration / design of the two sample return capsules (some of which are due to those considerations previously discussed that are not accounted for in the active vehicle model) as well as the highly conservative margins in the Stardust forebody TPS design (which resulted in significant margin in the TPS thickness, not duplicated in the MMEEV TPS sizing model).

The reduction in payload mass fraction between the passive and active architectures (~10%) is also shown. In addition, the difference in the entry ballistic coefficients between the architectures is also significant. The ballistic coefficient is

**Table 3. Case Study: Passive vs. Active Vehicle Architecture (0.8 m diameter vehicle and 13 kg payload)**

Parameter	Passive	Active	Stardust
Landing Condition	1500 g	4.6 m/s	4.6 m/s
Payload Mass Fraction	0.39	0.35	0.28
Entry Mass	33.5 kg	37.1 kg	45.8 kg
Impact or Parachute System Mass	2.5 kg	4.1 kg	4.2 kg
Entry Ballistic Coefficient	$\beta$	1.11 $\beta$	1.37 $\beta$

<sup>3</sup> A 13 kg payload mass was assumed based on the Stardust SRC total mechanism mass of 17.2 kg.



often used to gauge the expected aerothermal environments for a given vehicle configuration during the early (hypersonic) entry phase (e.g. the lower the ballistic coefficient, the lower the heating). When comparing the passive architecture to the active, the addition of the parachute system increases the ballistic coefficient by ~11%, resulting in a likely increase in the entry heating environment (which could result in larger TPS thicknesses, thus further adding to the vehicle entry mass, also requiring an even larger parachute, etc., etc.; none of which is being considered here). With this case study, for the active vehicle to achieve the same ballistic coefficient as the passive vehicle while keeping the same diameter and entry mass, the payload mass would need to be reduced by ~2.4 kg (18%), resulting in a reduced payload mass fraction of 0.32. Likewise, for the active vehicle to achieve the same ballistic coefficient as the passive vehicle while keeping the same payload mass, the vehicle diameter would need to increase to ~0.87 m, which would also increase the vehicle entry mass to ~39.7 kg, also resulting in a decrease in the payload mass fraction to 0.32.

## 9. CONCLUSIONS AND FUTURE WORK

When selecting between two alternative sample return vehicle architectures, passive and active (with a parachute), many factors must be considered. For any sample return mission, the ultimate determination of the payload landing requirement will be driven by science considerations (e.g. sample preservation). If the science can be preserved while still allowing for the payload (and/or sample) to experience high landing loads (> 1000 g), the passive approach appears to provide additional benefits over the parachute architecture by way of increased payload mass fraction, reduced vehicle complexity, reduced risk, and increased system reliability. Conversely, if the landing velocity requirement is low (< 5 m/s), a parachute system, not surprisingly, is the best approach. When considering higher landing velocities (> 10 m/s) or lower landing loads (< 1000 g), there appears to be little difference in the payload mass fraction between the passive and active architectures. In this range, the parachute system mass decreases to a point where it becomes comparable to an equivalent impact system. Under these circumstances, other considerations must be made, including environmental effects on landing performance in areas such as the landing footprint, vehicle configuration and complexity, risk and reliability, all of which can drive the overall development and testing costs of the vehicle. These more qualitative aspects have only been touched upon here, and finding better ways to quantify these could greatly aid in developing a tool to effectively trade these EEV architectures. In addition, as resources allow, further development of the MMEEV concept, including increased fidelity of the M-SAPE models, particularly in capturing the full effects of implementation of a parachute system, will be a focus in future work.

## SYMBOLS AND NOTATION

$(C_dS)_{mp}$	reference drag area of main parachute
$(C_dS)_v$	reference drag area of vehicle suspended from main parachute
$D_v$	vehicle diameter
$g$	acceleration due to gravity at the surface
$l_i$	landing load
$m_d$	drogue parachute mass
$m_{e_{active}}$	active (parachute) vehicle entry mass
$m_{e_{passive}}$	passive vehicle entry mass
$m_{is}$	impact system mass
$m_m$	mortar system mass
$m_{mp}$	main parachute mass
$m_{ps}$	total parachute system mass
$m_{pay}$	payload mass
$m_v$	vehicle mass
$\rho$	density of air at Earth's surface
$v_{term}$	terminal (landing) velocity

## ACKNOWLEDGEMENTS

The authors would like to thank all of those who have supported the development of the MMEEV concept and the M-SAPE tool over the past decade, the list of which is much too long to include here. Special thanks goes to NASA's Langley Research Center and Ames Research Center management, as well as NASA's In-Space Propulsion Technology Program, for their support, in the form of both encouragement and resources, to the development of this concept. Special thanks also go to all of those who have directly supported this research, particularly Cole Kazemba, Richard Winski, and Sotiris Kellas.

## REFERENCES

- [1] Mitcheltree R. A. et al. (2001), AAF Paper ARVS-102, *An Earth Entry Vehicle for Returning Samples From Mars*, 2<sup>nd</sup> International Symposium on Atmospheric Reentry Vehicles and Systems.

- [2] Maddock R. W. et al. (2008), *Multi-Mission Earth Entry Vehicle Design Trade Space and Concept Development Strategy*, IPPW6 (presentation).
- [3] Maddock R. W. et al. (2010), *Multi-Mission Earth Entry Vehicle Design Trade Space and Concept Development Status*, IPPW7 (presentation).
- [4] Maddock R. W. et al. (2011), *Multi-Mission Earth Entry Vehicle Design Trade Space and Concept Development Status Version 2.0*, IPPW8 (poster session).
- [5] Maddock R. W. et al. (2010), *An Application of the Multi-Mission Earth Entry Vehicle: Galahad – An Asteroid Sample Return Mission*, IPPW7 (poster session).
- [6] Samareh J. A. et al. (2014), *Multi-Mission System Analysis for Planetary Entry (M-SAPE) Version 1*, NASA/TM-2014-218507.
- [7] Kellas S., Mitcheltree R. A. (2002), *Energy Absorber Design, Fabrication and Testing for a Passive Earth Entry Vehicle*, AIAA-2002-1224.
- [8] Fasanella, E. L. et al. (2001), *Low Velocity Earth-Penetration Test and Analysis*, AIAA-2001-1388.
- [9] Knacke T. W. (1992), *Parachute Recovery Systems Design Manual*, pg. 6-95, Table 6-2.
- [10] Knacke T. W. (1992), *Parachute Recovery Systems Design Manual*, pg. 5-3, Table 5-1.
- [11] Knacke T. W. (1992), *Parachute Recovery Systems Design Manual*, pg. 6-96.
- [12] Christian J. A. et al. (2006), *Sizing of an Entry, Descent, and Landing System for Human Mars Exploration*, Space 2006 AIAA 2006-7427
- [13] F.W. Leslie, C.G. Justus (2011), *The NASA Marshall Space Flight Center Earth Global Reference Atmospheric Model – 2010 Version*, NASA/TM-2011-216467.
- [14] Eagle Engineering, Inc. (1988), *Risk Analysis of Earth Return Options for the Mars Rover/Sample Return Mission*, NASA-CR-172081.

## BIOGRAPHIES



**Robert Maddock** is a senior engineer in the Atmospheric Flight and Entry Systems Branch at NASA Langley Research Center. He received his Bachelor's degree in Aerospace Engineering from Parks

College of St. Louis University in 1992, and then went on to receive a Master's degree in Aerospace Engineering from The University of Tennessee Space Institute in 1995. In 1996 he joined the Jet Propulsion Laboratory where he worked in mission and trajectory design and systems engineering on several flight projects, including Cassini, the Shuttle Radar Topography Mission, and the Mars Science Laboratory (MSL). He also spent over five years in the Mars Advanced Studies Office supporting Mars Sample Return (MSR) mission studies and technology development. In 2005, Rob joined NASA Langley where he has provided simulation and development support for MSL and the ALHAT technology project, supported the development of the Autonomous Aerobraking Development Software system, leads Multi-Mission Earth Entry Vehicle technology and systems analyses for sample return missions, and currently acts as the Langley Entry Descent and Landing lead for the Mars InSight lander mission. He is a senior member of the AIAA.



**Allen Henning** is a senior at Virginia Polytechnic Institute and State University, pursuing a bachelor's of science degree in Aerospace Engineering. He conducted research last summer for the Langley Aerospace Research Student Scholars (LARSS) program and continued that research this summer for the NASA Internships, Fellowships, and Scholarships (NIFS) program. He is planning on attending graduate school at Virginia Polytechnic Institute and State University following his undergraduate studies.



**Jamshid Samareh** is a senior research aerospace engineer in the Vehicle Analysis Branch of NASA Langley Research Center. His research interests are in Entry and Descent Landing (EDL), mass modeling, multidisciplinary analysis and design optimization (MDO), fluid-structure interaction, geometry modeling, and shape optimization. He is the recipient of NASA Public Service Medal in 1995 and two-time winner of NASA Software of the Year Award as a member of TetrUSS team in 1996 and 2004. He was an Associate Editor of the AIAA Journal, a member of the AIAA MDO technical committee (TC) and is an associate fellow of the AIAA.